Lithuanian Journal of Physics, Vol. **46**, No. 1, pp. 53–61 (2006) doi:10.3952/lithjphys.46109

PHOTO- AND ELECTRO-REFLECTANCE STUDY OF δ-DOPED GaAs / AlAs MULTIPLE QUANTUM WELLS

J. Kavaliauskas [a], G. Krivaitė [a], B. Čechavičius [a], A. Galickas [a], G. Valušis [a], D. Seliuta [a], M.P. Halsall [b], M.J. Steer [c], and P. Harrison [d]

[a] *Semiconductor Physics Institute, A. Goštauto 11, LT-01108 Vilnius, Lithuania*
E-mail: jk@pfi.lt
[b] *Department of Electronics and Electrical Engineering, University of Manchester, P.O.B. 88, Manchester M60 1QD, UK*
[c] *Department of Electronic and Electrical Engineering, University of Sheffield, Mappin St, Sheffield S1 3JD, UK*
[d] *Institute of Microwaves and Photonics, School of Electronic and Electrical Engineering, University of Leeds, Leeds LS2 9JT, UK*

Received 12 October 2005

We present photoreflectance (PR) and contactless electroreflectance (CER) study of beryllium δ-doped GaAs / AlAs multiple quantum wells (MQWs) with well widths ranging from 3 to 20 nm and doping densities from $2{\cdot}10^{10}$ to $2.5{\cdot}10^{12}$ cm^{-2}. Surface electric field strength as well as its direction in MQW structures have been evaluated from PR and CER measurements. PR and CER spectra of heavily doped QWs were found to be more complicated than those of slightly doped ones. The interpretation of spectral features was performed on the basis of their dependence on the optical bias and from comparison with calculations of electronic structure and optical transitions under electric field. Modulation spectra of slightly doped samples were explained by symmetry allowed excitonic transitions while additional features in spectra of heavily-doped samples were related to symmetry forbidden transitions coming into play due to the internal electric field. The light interference and free carrier effects in modulation spectra are considered as well.

Keywords: δ-doped GaAs / AlAs multiple quantum wells, electroreflectance, photoreflectance

PACS: 78.67.De, 73.21.Fg, 78.55.Cr

1. Introduction

The increasing need for terahertz (THz) electronics has stimulated a great interest in a study of semiconductor nanostructures as possible active components for THz devices. Recently, a novel beryllium δ-doped GaAs / AlAs multiple quantum well (MQW) system has been proposed for this application [1–3]. The frequencies of optical transitions between sublevels of Be acceptors in δ-doped GaAs / AlAs MQW structures lie within the THz range, and the frequency can be tuned by varying the width of the well [4–6]. Therefore, such structures seem to be very attractive for fabrication of THz detectors and emitters. Evidently, in order to optimize the device design, the knowledge about material properties, internal electric fields, interface quality, doping effects, and various imperfections in QW structures is of essential importance. Such information may be obtained by modulation spectroscopy techniques, in particular, by non-destructive photoreflectance (PR) and contactless electroreflectance (CER) methods [7–9], that enable one to study QW structures with high spectral sensitivity even at room temperature. Some results concerning optical and electronic properties of beryllium δ-doped GaAs / AlAs MQW structures, obtained by PR and differential surface photovoltage (DSPV) [10] methods, were already presented in [11, 12]. In particular, the PR technique has been used for the study of these structures in order to determine the internal electric field and the energies of the QW-related optical transitions. However, some problems such as the location of the electric field region responsible for PR features, as well as the influence of the internal electric field on the optical transitions, are not solved up to now.

In this work, we have therefore focused ourselves into a study of internal electric field effect on interband optical transitions in beryllium δ-doped GaAs / AlAs MQW structures by application of the PR and CER techniques. From CER measurements, the surface electric field strength as well as its direction in GaAs / AlAs MQW structures has been evaluated. To

© Lithuanian Physical Society, 2006
© Lithuanian Academy of Sciences, 2006
ISSN 1648-8504

Table 1. Characteristics of the samples: the repeated period, the quantum well width (L_w), the δ-doping Be concentration (N_A), and the growth temperature of the epitaxial layer (T).

Samples	Periods	L_w (nm)	N_A (cm^{-2})	T (°C)
1795	400	3	$2{\cdot}10^{10}$	550
1794	200	10	$5{\cdot}10^{10}$	550
1303	50	15	$2.5{\cdot}10^{12}$	540
1392	40	20	$2.5{\cdot}10^{12}$	540
1807	100	20	$5{\cdot}10^{10}$	550
1796	5 μm thick GaAs epilayer		$2{\cdot}10^{16}$ cm^{-3}	550

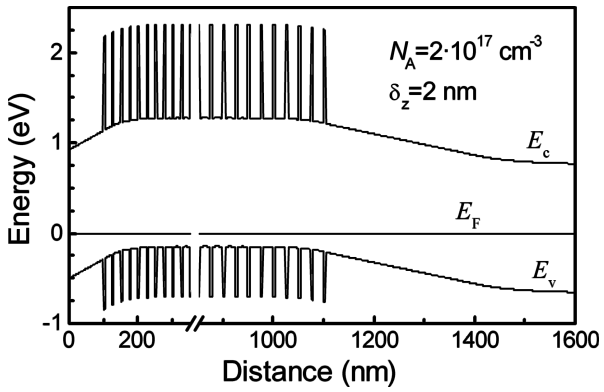

Fig. 1. Band diagram of Be δ-doped GaAs / AlAs MQW structure 1807.

identify the observed spectral features by optical transitions, we have investigated the behaviour of modulation spectra under optical bias and have calculated the electronic structure under the action of electric field.

2. Samples and experiment

A series of Be δ-doped GaAs / AlAs MQWs with the doping at the well centre as well as a single epilayer of GaAs:Be were grown by MBE on a semi-insulating (100) GaAs substrate in a VG V80H reactor equipment with all solid sources. Prior to the growth of the MQW, a GaAs buffer layer of 300 nm thickness was grown. Each of the investigated MQW structures contained the same 5 nm width AlAs barrier, while QW widths ranged from 3 to 20 nm and a doping level varied from $2{\cdot}10^{10}$ to $2.5{\cdot}10^{12}$ cm^{-2}. The doping level and main characteristics of each sample are summarized in Table 1. The schematic band diagram of δ-doped GaAs / AlAs MQW structures was calculated from Poisson equation and is shown in Fig. 1. It was assumed that the surface Fermi level for p-type GaAs is pinned at 0.5 eV above the valence band [13]. Consequently, this results in the formation of a surface depletion layer and a surface electric field. Another depletion layer is also formed at the interface between the MQW layer and the substrate due to Fermi level pinning near midgap of the semi-insulating GaAs.

The PR measurements were performed using a He–Ne laser (wavelength 632.8 nm) or a light emitting diode (LED) (wavelength 470 nm) light beams as the modulation pump sources. The penetration depth of the He–Ne and LED light beams into GaAs was estimated to be about 240 and 50 nm, respectively. The PR spectra were measured in phase with the modulated 650 Hz pump beam. Pump intensities were kept below 2 mW/cm^2.

For the CER studies, a condenser-like system was utilized [8, 12]. An ac modulation voltage in the range of 300–500 V was applied to the top transparent electrode to provide modulating field. Also, an additional steady state illumination of He–Ne laser was used as an optical bias to reduce the built-in electric field in the sample. The experimental conditions were chosen so that negative half-cycle of the voltage applied to the top electrode in CER measurements would correlate with illumination half-cycle on the sample in PR experiment. This was done in order to facilitate the comparison of the CER and PR signals and to evaluate the direction of surface band bending. It was found that under those measurement conditions CER and PR spectra exhibit the same (opposite) signs for bulk $p(n)$-type GaAs sample.

The PR and CER signals were recorded by a conventional lock-in detection system. The measurements were performed at room temperature.

3. Results and discussion

3.1. PR and CER spectra of lightly doped samples

Figure 2 shows room temperature PR spectra for an epitaxial p-GaAs layer and for the lightly doped GaAs / AlAs MQW structure with various well widths. The spectra are dominated by bulk-like signal arising in the vicinity of the GaAs fundamental gap E_g (1.424 eV) with the characteristic oscillations. These

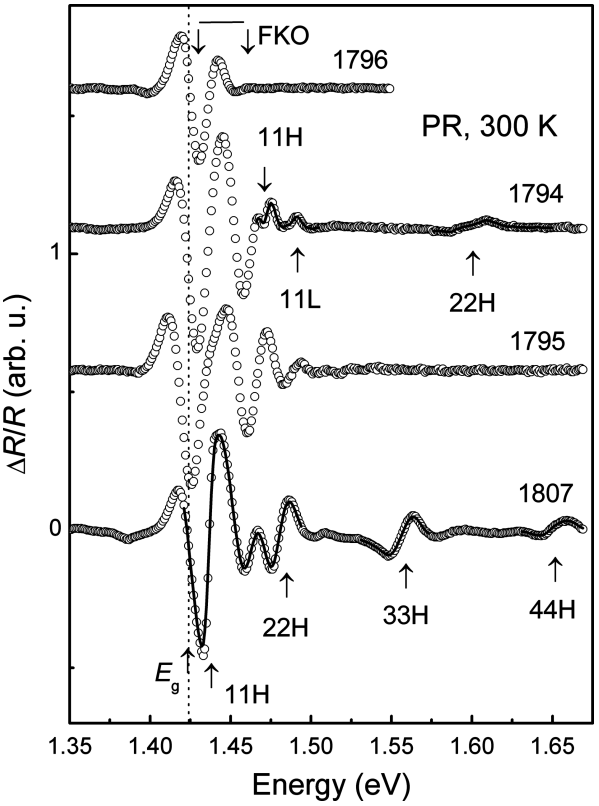

Fig. 2. Room temperature PR spectra of epitaxial p-GaAs layer and lightly Be δ-doped GaAs / AlAs MQW samples with various well widths. The transition energies indicated by arrows are obtained from the fit (solid lines) of a lineshape function (1) to the experimental data (open circles).

PR features were associated with Franz–Keldysh oscillations (FKOs) indicating the existence of the internal electric field in the samples. In addition, at higher energies, a number of mnH(L) features associated with the excitonic optical transitions in the MQW region of the samples are clearly observed. The notation mnH(L) signifies the transitions between the mth electron and nth heavy hole (H) or light hole (L) subbands. The energies and broadening parameters of optical transitions responsible for observed PR features (Fig. 2) were determined from the fit of the PR spectra to the derivative functional form proposed by Aspnes [14]:

$$\frac{\Delta R}{R} = \mathrm{Re}\left[C\mathrm{e}^{\mathrm{i}\theta}(E - E_\mathrm{g} + \mathrm{i}\Gamma)^{-m}\right], \qquad (1)$$

where C, θ, E_g, and Γ are amplitude, phase, energy, and broadening parameter of the spectral feature, respectively. The value of parameter $m = 3$ was used in the calculations. It should be noted that in this case the expression (1) quite well represents the first derivative of an excitonic dielectric function with a Gaussian absorption profile [7, 15], and that is appropriate for quantum systems with inhomogeneously broadened energy levels.

The energies of optical transitions, denoted by arrows in Fig. 2, change according to the QW thickness as expected from the quantum confinement effect. For large well width samples, 1807, 1303, and 1392, the intense ground state QW transitions occur rather close in energy to the GaAs band gap. Therefore, bulk-like FKO signals were not well resolved in the PR spectra of these samples.

Internal electric fields. Further, we will discuss the origin of the FKOs above the GaAs band gap. According to the calculated band diagram (Fig. 1), these FKOs may originate from photo-modulation of the band bending near the surface in the GaAs cap layer, and / or near the interface in the GaAs buffer layer. In order to identify the location of electric field region responsible for FKOs in the PR spectra, we performed CER measurements since the sign (phase) of CER features near the GaAs band gap energy contains the information on the sign or direction of electric field [16]. A comparison of the CER spectra for p-GaAs epilayer 1796 and GaAs / AlAs MQW sample 1795 is shown in Fig. 3(a). Therein, the PR spectra for these samples are also presented. As can be seen from Fig. 3(a), the phase of the CER signal is the same both for the p-type GaAs epitaxial layer 1796 and for GaAs / AlAs MQW sample 1795. This result suggests that near the surface the electric field region with downward band bending at the topmost layers (Fig. 1) must be mainly responsible for electro- and photo-modulated signals from GaAs / AlAs MQW structures. It should be noted that the FKOs period for PR spectra is significantly smaller than that in CER spectra (Fig. 3(a)). This is related to the decrease of the surface electric field under illumination by the laser beam during PR measurements. Also, taking into account the band diagram depicted in Fig. 1, δ-doped MQW structures should exhibit nearly uniform electric field in the undoped GaAs cap layer and cause slowly decaying FKOs in the PR and CER spectra. In contrast, due to non-uniform electric field and the broadening effects in a doped epitaxial GaAs layer, the FKOs are damped much faster (Fig. 3(a)).

By analysing the FKOs above the GaAs band edge it is possible to calculate the surface electric field. In the analysis of the electric field strength, the oscillating behaviour of FKOs is described as [17]

$$\frac{\Delta R}{R} \sim \cos\left\{\frac{4}{3}\cdot\left[\frac{E - E_\mathrm{g}}{\hbar\Omega}\right]^{3/2} + \varphi\right\}, \qquad (2)$$

where E is the photon energy, $E_{\rm g}$ denotes the band gap energy, $\hbar\Omega = [e^2F^2\hbar^2/(8\mu)]^{1/3}$ is an electro-optic energy (e stands for the electron charge, μ marks the reduced mass of the electron and hole in the direction of the electric field F, $\hbar$ labels Planck constant), and φ is a phase factor. In accordance with Eq. 2, the extremes of the FKOs are given by

$$n\pi = \frac{4}{3}\cdot\left[\frac{E_n - E_{\rm g}}{\hbar\Omega}\right]^{3/2} + \varphi\,, \qquad (3)$$

where n is the index of the nth extremum, E_n denotes the photon energy of the nth oscillation, and $E_{\rm g}$ marks the band gap of GaAs. In Fig. 3(b), the quantity $[4/(3\pi)](E_n - E_{\rm g})^{3/2}$ versus index n is plotted. The solid lines show linear fit to Eq. (3). From the slope of these lines it was possible to evaluate the electro-optic energy $\hbar\Omega$ and, hence, the built-in electric field strength. For GaAs, the effective masses of electron and heavy hole equal to $0.065\,m_0$ and $0.34\,m_0$, respectively, were used in the calculations. The obtained spectroscopic values of the electric field F are presented in Fig. 3(b). As is seen, in agreement with considered peculiarities of the samples and FKOs, the surface electric field in MQW structures exceeds that in doped epitaxial layer. Also, due to flattening of band bending under illumination of the sample, the built-in electric field determined from PR is smaller than that estimated from CER spectra. The surface electric field values of the MQW structures are of about 20 kV/cm and are consistent with the calculated surface field value (Fig. 1) for acceptor concentration of $2{\cdot}10^{17}$ cm^{-3}.

3.2. PR and CER spectra of highly doped samples

Further, we employed the CER and PR techniques to study the effects of electric field on the optical transitions in MQW region of highly doped samples. CER and PR spectra for sample 1303 are displayed in Fig. 4. For comparison, the DSPV spectrum is also shown. It actually represents the first derivative of the transmission spectrum of MQW layers, as described elsewhere [11]. The sharp derivative-like features are seen in DSPV spectrum above the GaAs band edge at 1.424 eV. According to our calculations of the subband energies [11], these features are attributed to allowed excitonic interband transitions 11H, 22H and 33H.

Consideration of CER and PR spectra allows one to note the following peculiarities. First of all, the polarity of the CER and PR lines is the same, thus indicating that the signals are mostly controlled by the surface electric field penetrating into the MQW region (Fig. 1).

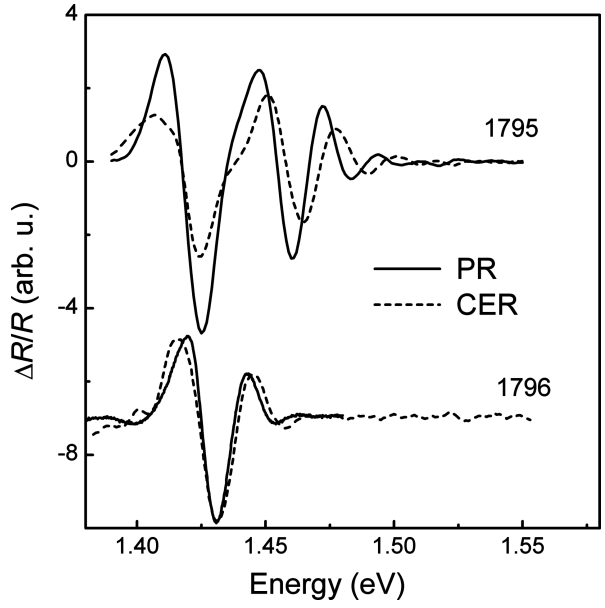

(a)

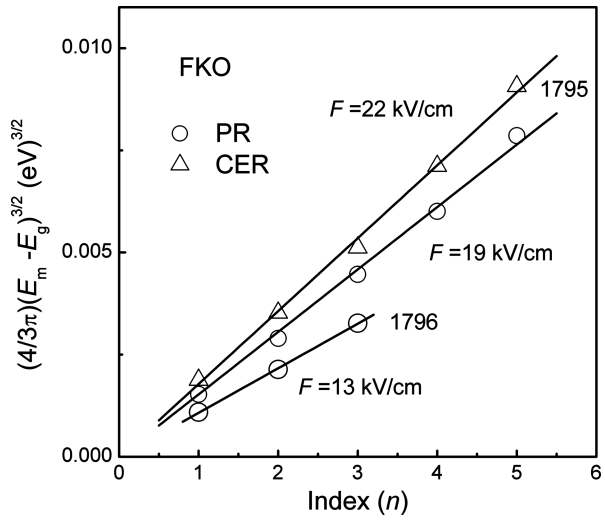

(b)

Fig. 3. (a) Comparison of the PR and CER spectra and (b) plots of the quantity $[4/(3\pi)](E_n - E_{\rm g})^{3/2}$ versus index n of Franz–Keldysh oscillations for epitaxial p-GaAs layer 1796 and GaAs / AlAs MQW sample 1795.

Another important peculiarity of CER and PR spectra, clearly seen in Fig. 4, comes from the fact that these spectra are more complicated than the DSPV and PR spectra for lightly doped samples (Fig. 2). In description of the complicated lineshape of CER and PR spectra by expression (1), the additional features denoted in Fig. 4 by mnH ($m \neq n$) should be included. These features are hardly observable in DSPV and PR spectra of slightly doped samples (Fig. 2).

By interpreting these extra features, it is worth to mention that they are observed in the range of higher order optical transitions with energies that are rather in-

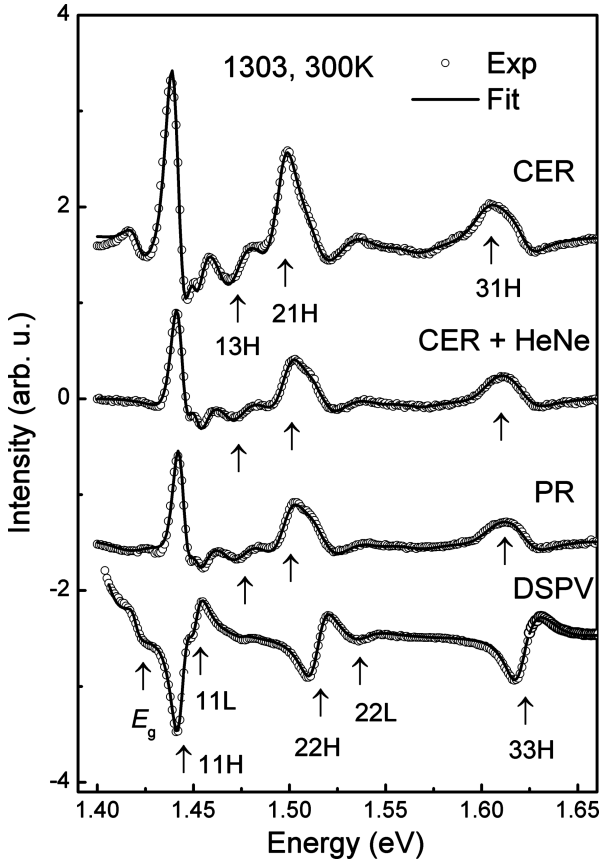

Fig. 4. CER spectrum of heavily δ-doped GaAs / AlAs MQW structure 1303 measured with and without optical bias. PR and DSPV spectra are also shown for comparison. The transition energies indicated by arrows are obtained from the fit (solid lines) of a lineshape function (1) to the experimental data (open circles).

sensitive to the electric field strength. Thus, they cannot be attributed to the effect of the spatial variation of the electric field across the QWs in the surface depletion region leading to the splitting of the optical features via quantum confined Stark effect [18]. Therefore, we believe that the other origin of the observed spectral features should be considered in more detail. The first one is the light interference phenomenon, sometimes leading to similar shoulders to the peaks in the CER spectra of the MQW structures [19]. Second possibly responsible effect can be the breaking of the normal ($\Delta n = 0$) selection rules for optical transitions in the electric field. As a consequence, usually symmetry forbidden transitions may give then some additional spectral peculiarities [20].

To disclose the origin of discussed features, we checked the possibility of light interference effects by measuring CER spectra with the probe beam incident at 15° and 60° angles. However, we found no spectral shift of CER features due to enhanced optical path of light beam. This reveals that the considered CER features cannot be correctly explained by light interference effects.

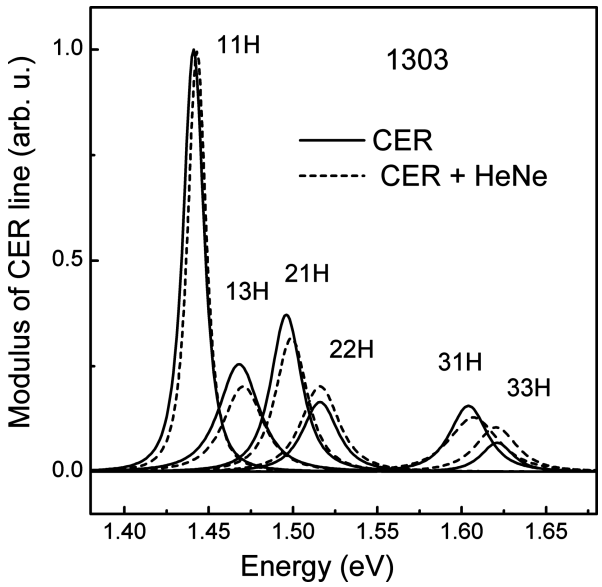

Fig. 5. CER modulus spectra for δ-doped GaAs / AlAs MQW structure 1303. CER modulus amplitudes are normalized to that of 11H.

Thus, it is very likely that additional features appearing in CER and PR spectra can be related to normally forbidden transitions. Usually, the appearance of the forbidden excitonic transitions in the spectra of QWs can be due to structural assymetry or an electric field induced relaxation of the selection rules for optical transitions [7].

In order to grasp whether the built-in electric field is responsible for the origin of observed features, CER measurements under steady illumination of the sample by He–Ne laser beam were performed. It was found that optical bias, as was known previously, decreased the magnitude of surface electric field; therefore, the CER spectra experienced significant changes and became almost identical to PR ones (Fig. 4). These changes are best seen by considering the CER modulus spectra (Fig. 5) evaluated from the CER resonances according to [21]:

$$|\Delta\rho(E)| = \frac{C}{\left[(E - E_{\rm ex})^2 + \Gamma^2\right]^{m/2}}\,. \qquad (4)$$

It should be noted that the position of the peaks in the CER modulus spectra corresponds to optical transition energy while their height is proportional to intensity of the transition. Unfortunately, the optical bias reduces not only the dc electric field but also the ac modulating field strength [22], resulting in diminishing of all CER features (Fig. 4). Therefore, we cannot directly attribute the changes in amplitude of experimental CER features

under illumination to changes in optical transition intensity. In such a case only relative intensity of different optical transitions in the spectra should be compared. In order to facilitate such a comparison, the CER modulus amplitudes in Fig. 5 are normalized to that of 11H. Figure 5 clearly demonstrates that with decreasing surface electric field by optical bias, the spectral features related to various types of optical transitions reveal different changes in their spectral position and relative intensity. These facts suggest that the additional CER and PR features are influenced by the surface electric field and can be explained by the $\Delta n \neq 0$ forbidden interband transitions. We suppose that the considered features were not clearly resolved in PR spectra of lightly doped samples (Fig. 2) due to weaker surface electric field (larger Debye's screening length) and, probably, smaller distortion of potential profile by the δ-planes in QWs. More detailed interpretation of optical data was performed on the basis of calculations of GaAs / AlAs QWs subband structure under electric field.

3.3. Optical transitions under electric field

Calculations of subband structure. To identify the observed spectral features and to explain their dependences on the surface electric field, calculations of energy levels and interband transition energies under electric field for GaAs / AlAs QWs have been carried out by the transfer matrix method [23]. The overlap integrals of electron and heavy (light) hole wave functions have also been estimated. The conduction band offset was taken to be 0.65 . We used the parameters of GaAs and AlAs employed in our previous work [11]. In calculations, we assumed the rectangular potential profile of QW in the absence of electric field. To check this assumption, we have performed the calculations of energy levels by solving the coupled Poisson–Schrödinger equations. It was found that the change in the ground state optical transition energy due to distortion of the rectangular potential profile by δ-doping is negligible and reaches ≤ 3 meV when the concentration of acceptors is $2.5{\cdot}10^{12}$ cm^{-2} and the width of the QW is 20 nm. For narrower QWs and higher-order optical transitions the deviations were found to be even smaller.

It is worth noting that the calculations of subband structure by solving the coupled Poisson–Schrödinger equation have shown that at room temperature the QWs with the acceptor concentration of $2.5{\cdot}10^{12}$ cm^{-2} should be non-degenerate. The critical impurity concentration for Mott transition to semimetalic state, $N_{\rm cr}$, approximately evaluated by the relation $N_{\rm cr} = 0.097\, a_{\rm B}^{-2}$ [24], where $a_{\rm B}$ is the impurity Bohr radius, for δ-doped GaAs / AlAs QWs with the thicknesses of 15 and 20 nm was found to be about $3{\cdot}10^{12}$ cm^{-2}. This also does not contradict the proposition as to the non-degeneracy of heavily doped QWs under consideration. Besides that, the far-infrared absorption measurements of the same GaAs / AlAs QWs [5] clearly show absorption lines due to transitions between the ground and excited Be states both in lightly and heavily δ-doped samples. This indicates that the doping density in our samples is below the level needed for formation of impurity bands that close all gaps and smear out the absorption lines.

Figure 6(a) shows the calculated electric field dependences of Stark shifts of interband transition energies in 1303 MQW sample. As is seen, with increasing electric field, various optical transitions exhibit Stark shifts of different direction and magnitude, which favours their identification. The largest red shift (towards lower energies) reveals ground state transition 11H and other higher energy transitions (21H, 31H) involving heavy hole ground state 1H which has the largest field-induced shift of any of the levels. At the same time, almost all other transitions at small electric fields exhibit negligible blue shift (towards higher energies) while at sufficiently high fields, in contrast, they show red Stark shift.

While identifying the spectral features by various optical transitions it is important to consider their oscillator strengths which are proportional to the squares of the overlap integrals between the electron and hole wavefunctions, $|M_{\rm cv}|^2$. Figure 6(b) illustrates the calculated electric field dependence of $|M_{\rm cv}|^2$ for various optical transitions in 1303 MQW sample. As is seen, the overlap integral between the electron and hole wavefunctions for allowed transitions 11H gradually diminishes with electric field. For 22H and 33H transitions, the $|M_{\rm cv}|^2$ decreases with electric field up to sufficiently high fields reaching about 70 kV/cm and, further, begins to increase. On the contrary, for partly symmetry forbidden transitions such as 21H, 32H etc., the $|M_{\rm cv}|^2$ at small electric fields increases with field while at high fields it diminishes. Such behaviour of overlap integrals reveals a redistribution of oscillator strengths of optical transitions in electric field, namely, their transfer from allowed transitions to forbidden ones.

Identification of spectral features. On the basis of these calculations, the features in PR and CER spectra were identified by symmetry allowed and forbidden optical transitions indicated in Fig. 5. As is seen, with decreasing the surface electric field by optical bias, the dominant low energy excitonic feature 11H in CER

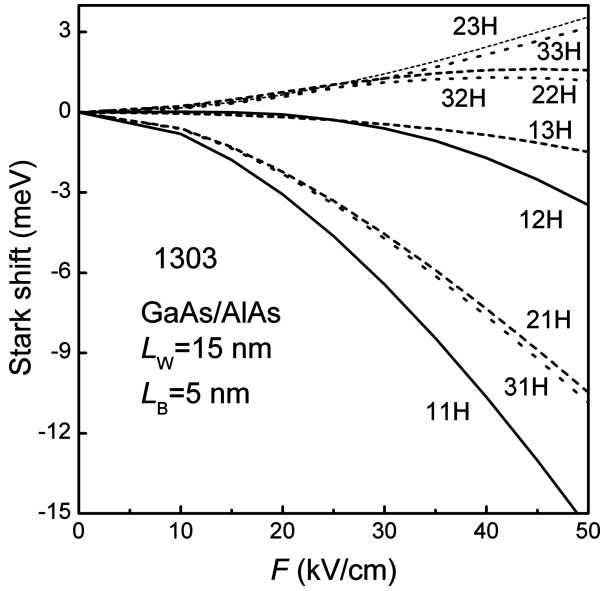

(a)

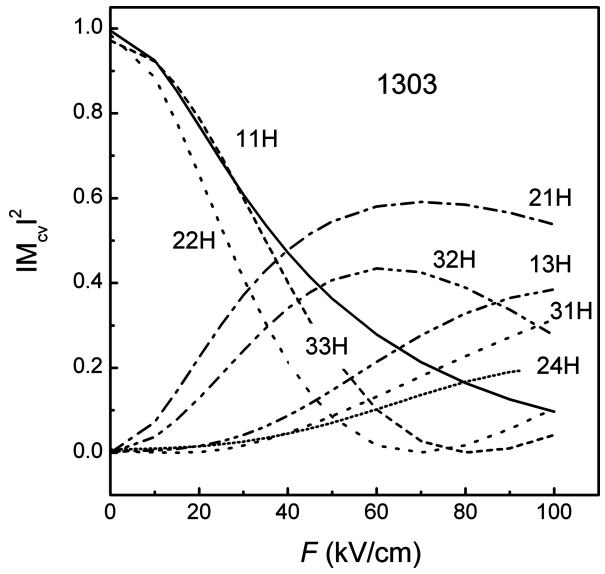

(b)

Fig. 6. (a) Calculated electric field dependences of Stark shifts of interband transition energies and (b) the squares of the overlap integrals between the electron and hole wavefunctions, $|M_{cv}|^2$, for GaAs / AlAs MQW structure 1303.

modulus spectra exhibits usual blue shift in accordance with Fig. 6(a), which, as expected, was found to be larger for the sample 1392 with larger QW width. At the same time, the spectral positions of allowed higher energy transitions 22H and 33H, including excited states, were observed almost not to change with optical bias (Fig. 5), as calculations revealed (Fig. 6(a)). The observed shift of forbidden transitions 21H, 31H, and 13H to higher energies with optical bias also correlates with calculations.

By considering the behaviour of intensities of CER features under optical bias (Fig. 5) we cannot directly relate them to oscillator strengths of optical transitions, because the amplitude of the modulated excitonic reflectance depends on a number of experimental factors. In addition, changes under external modulation occur not only in oscillator strength, but also in exciton energy and line broadening. Nevertheless, the examination of CER modulus spectra (Fig. 5) has revealed that the ratio of CER intensities due to forbidden and allowed transitions tends to decrease with reducing built-in electric field by optical bias. This experimental observation correlates with calculated field dependences of overlap integrals (Fig. 6(b)), which are proportional to oscillator strength of optical transitions, and confirms the proposed interpretation of optical data.

Finally, it should be noted that in heavily doped QWs another modulation mechanism such as state-filling modulation [8] might give contribution to PR and CER signals. Indeed, the decrease of surface band bending with optical bias should be accompanied by some increase in population of hole subbands in QW. In particular, it can be attributed to the lowest one, 1H, which should be nearest to the Fermi level (Fig. 1). This, in turn, should result in the decrease in oscillator strength of excitonic transitions including these subbands. Although this effect may have influence on 11H and other 1H-related PR and CER features, it is hardly expected to be dominant in studied nondegenerate QWs. On the other hand, the increase of doping density was found to slightly enhance the exciton line broadening parameter Γ, which was studied in more detail in our previous work [11].

4. Conclusions

The photoreflectance (PR) and contactless electroreflectance (CER) spectroscopies have been used to study optical transitions and electronic structure as well as internal electric fields of Be δ-doped GaAs / AlAs MQWs with their widths ranging from 3 to 20 nm and a doping level from $2{\cdot}10^{10}$ to $2.5{\cdot}10^{12}$ cm^{-2}. From the analysis of FKOs in CER and PR spectra, the surface electric field values in lightly doped MQW structures are estimated to be of about 20 kV/cm. We have interpreted the PR and CER spectra using their changes while varying the optical bias and comparing them with the calculations of electronic structure and optical transitions under electric field. The PR and CER spectra of slightly doped samples were explained by symmetry allowed excitonic transitions while additional features in spectra of heavily doped samples were found to be related

to symmetry forbidden transitions gaining their strength with electric field. The influence of state-filling modulation of hole subbands on CER signal in heavily doped QWs is also considered.

References

[1] P. Harrison, M.P. Halsall, and W.-M. Zheng, Quantum-confined impurities as single-electron quantum dots: Application in terahertz emitters, Mater. Sci. Forum **384–385**, 165–172 (2002).

[2] P. Harrison and R.W. Kelsall, Population inversion in optically pumped asymmetric quantum well lasers, J. Appl. Phys. **81**(11), 7135–7140 (1997).

[3] M.P. Halsall, P. Harrison, J.-P. Wells, I.V. Bradley, and H. Pellemans, Picosecond far-infrared studies of intra-acceptor dynamics in bulk GaAs and δ-doped AlAs / GaAs quantum wells, Phys. Rev. B **63**(15), 155314–155318 (2001).

[4] W.M. Zheng, M.P. Halsall, P. Harmer, P. Harrison, and M.J. Steer, Acceptor binding energy in δ-doped GaAs / AlAs multiple-quantum wells, J. Appl. Phys. **92**(10), 6039–6042 (2002).

[5] W.M. Zheng, M.P. Halsall, P. Harrison, J.-P.R. Wells, I.V. Bradley, and M.J. Steer, Effect of quantum-well confinement on acceptor state lifetime in δ-doped GaAs / AlAs multiple quantum wells, Appl. Phys. Lett. **83**(18), 3719–3721 (2003).

[6] W.M. Zheng, M.P. Halsall, P. Harmer, P. Harrison, and M.J. Steer, Effect of quantum confinement on shallow acceptor transitions in δ-doped GaAs / AlAs multiple-quantum wells, Appl. Phys. Lett. **84**(5), 735–737 (2004).

[7] O.J. Glembocki and B.V. Shanabrook, Photoreflectance spectroscopy of microstructures, in: *Semiconductors and Semimetals*, Volume 36, eds. D.G. Seiler and C.L. Littler (Academic Press, San Diego, 1992) pp. 221–292.

[8] F.H. Pollak and H. Shen, Modulation spectroscopy of semiconductors: Bulk / thin film, microstructures, surfaces / interfaces and devices, Mater. Sci. Eng. R **10**(7–8), 275–374 (1993).

[9] J. Misiewicz, P. Sitarek, G. Sęk, and R. Kudrawiec, Semiconductor heterostructures and device structures investigated by photoreflectance spectroscopy, Mater. Sci. (Poland) **21**(3), 263–320 (2003).

[10] Y.S. Huang and F.H. Pollak, Non-destructive, room temperature characterization of wafer-sized III-V semiconductor device structures using contactless electromodulation and wavelength-modulated surface photovoltage spectroscopy, Phys. Status Solidi A **202**(7), 1193–1207 (2005).

[11] B. Čechavičius, J. Kavaliauskas, G. Krivaitė, D. Seliuta, G. Valušis, M.P. Halsall, M.J. Steer, and P. Harrison, Photoreflectance and surface photovoltage spectroscopy of beryllium-doped GaAs / AlAs multiple quantum wells, J. Appl. Phys. **98**(2), 023508(8) (2005).

[12] B. Čechavičius, J. Kavaliauskas, G. Krivaitė, D. Seliuta, E. Širmulis, J. Devenson, G. Valušis, M.P. Halsall, M.J. Steer, and P. Harrison, Optical and terahertz characterization of Be-doped GaAs / AlAs multiple quantum wells, Acta Phys. Pol. A **107**(2), 328–332 (2005).

[13] S.M. Sze, *Physics of Semiconductor Devices*, 2nd ed. (Wiley, New York, 1981).

[14] D.E. Aspnes, Third-derivative modulation spectroscopy with low-field electroreflectance, Surf. Sci. **37**, 418–442 (1973).

[15] B.V. Shanabrook, O.J. Glembocki, and W.T. Beard, Photoreflectance modulation mechanism in GaAs / $Al_xGa_{1-x}As$ multiple quantum wells, Phys. Rev. B **35**(5), 2540–2543 (1987).

[16] X. Yin, X. Guo, F.H. Pollak, G.D. Pettit, J.M. Woodal, T.P. Chin, and C.W. Tu, Nature of band bending at semiconductor surface by contactless electroreflectance, Appl. Phys. Lett. **60**(11), 1336–1338 (1992).

[17] D.E. Aspnes and A.A. Studna, Schottky-barrier electroreflectance: Application to GaAs, Phys. Rev. B **7**(10), 4605–4625 (1973).

[18] O. Mayrock, H.-J. Wünsche, and F. Henneberger, Polarization charge screening and indium surface segregation in (In,Ga)N / GaN single and multiple quantum wells, Phys. Rev. B **62**(24), 16870–16880 (2000).

[19] A.J. Shields and P.C. Klipstein, Line-shape model for the modulated reflectance of multiple quantum wells, Phys Rev. B **43**(11), 9118–9125 (1991).

[20] K. Satzke, G. Weiser, W. Stolz, and K. Ploog, Optical study of electronic states of $In_{0.53}Ga_{0.57}As$ / $In_{0.52}Al_{0.48}As$ quantum wells in high electric fields, Phys. Rev. B **43**(3), 2263–2271 (1991).

[21] R. Kudrawiec, G. Sęk, K. Ryczko, J. Misiewicz, and J.C. Harmand, Photoreflectance investigations of oscillator strength and broadening of optical transitions for GaAsSb–GaInAs / GaAs bilayer quantum wells, Appl. Phys. Lett. **84**(18), 3453–3455 (2004).

[22] S.L. Mioc, J.W. Garland, and B.R. Bennet, Charge trapping and built-in field studies in electroreflectance of a UN+ GaAs structure, Semicond. Sci. Technol. **11**(4), 521–524 (1996).

[23] B. Jonsson and S.T. Eng, Solving the Shrödinger equation in arbitrary quantum well profiles using the transfer matrix method, IEEE J. Quantum Electron. **26**(11), 2025–2035 (1990).

[24] J. Kortus and J. Monecke, Formation of subbands in δ-doped semiconductors, Phys. Rev. B **49**(24), 17216–17223 (1994).

δ LEGIRUOTŲ GaAs / AlAs KVANTINIŲ DUOBIŲ FOTOATSPINDŽIO IR ELEKTRINIO ATSPINDŽIO SPEKTRŲ TYRIMAI

J. Kavaliauskas [a], G. Krivaitė [a], B. Čechavičius [a], A. Galickas [a], G. Valušis [a], D. Seliuta [a], M.P. Halsall [b], M.J. Steer [c], P. Harrison [d]

[a] *Puslaidininkių fizikos institutas, Vilnius, Lietuva*
[b] *Mančesterio universitetas, Mančesteris, Jungtinė Karalystė*
[c] *Šefildo universitetas, Šefildas, Jungtinė Karalystė*
[d] *Lydso universitetas, Lydsas, Jungtinė Karalystė*

Santrauka

Priemaišinių lygmenų δ legiruotose kvantinėse duobėse inžinerija atveria naujų galimybių kurti terahercinių bangų emiterius bei detektorius. Nanodarinių tyrimas nesąlytiniais optiniais metodais yra svarbus, norint suprasti tokių prietaisų veikimo ypatumus. Pasitelkus fotoatspindžio ir elektrinio atspindžio spektroskopijos metodus, buvo tiriama beriliu δ legiruotų ($2{\cdot}10^{10}$ – $2{,}5{\cdot}10^{12}$ cm^{-2}) GaAs / AlAs (3–20 nm/5 nm) kvantinių duobių darinių elektroninė sandara ir legiravimo poveikis eksitoniniams optiniams šuoliams bei vidiniams elektriniams laukams.

Išanalizavus moduliacinių atspindžio spektrų linijų formą bei apskaičiavus energijos lygmenis kvantinėse duobėse, pastebėtos optinių spektrų smailės buvo susietos su leistinais bei draustinais eksitoniniais šuoliais. Optinių smailių interpretacija buvo patvirtinta, ištyrus jų energijų bei intensyvumų verčių priklausomybes nuo vidinio elektrinio lauko stiprio. Nustatyta, jog silpnai legiruotų bandinių spektruose vyrauja leistini optiniai šuoliai, o stipriai legiruotiems bandiniams yra būdingi ir draustini optiniai šuoliai, kurių intensyvumas stiprėja, stiprėjant elektriniam laukui. Paaiškinta, kad fotoatspindžio ir elektrinio atspindžio signalų prigimtis beriliu δ legiruotų GaAs / AlAs kvantinių duobių dariniuose priklauso nuo vidinio elektrinio lauko moduliacijos. Eksperimentiškai nustatytas šio lauko stipris bei kryptis bandiniuose.

Taip pat aptarta šviesos interferencijos ir laisvųjų krūvininkų įtaka elektromoduliaciniams spektrams.